NAA–SR–7368

SNAP SHIELD TEST EXPERIMENT

REACTOR PHYSICS TESTS

AEC Research and Development Report

ATOMICS INTERNATIONAL
A DIVISION OF NORTH AMERICAN AVIATION, INC.

DISCLAIMER

Price $0.75
Available from the Office of Technical Services
Department of Commerce
Washington 25, D. C.

NAA-SR-7368
PHYSICS
35 PAGES

SNAP SHIELD TEST EXPERIMENT

REACTOR PHYSICS TESTS

By
R. L. TOMLINSON *
R. P. JOHNSON
S. G. WOGULIS

*Present Address: Aerojet General Nucleonics
P.O. Box 77
San Ramon, California

ATOMICS INTERNATIONAL

A DIVISION OF NORTH AMERICAN AVIATION, INC.
P.O. BOX 309 CANOGA PARK, CALIFORNIA

CONTRACT: AT(11-1)-GEN-8
ISSUED: JUL 15 1962

DISTRIBUTION

This report has been distributed according to the category "Physics" as given in "Standard Distribution Lists for Unclassified Scientific and Technical Reports" TID-4500 (16th Ed.), December 15, 1960. A total of 670 copies was printed.

CONTENTS

TABLES

FIGURES

ABSTRACT

The initial physics tests on the Shield Test Experiment reactor and the precriticality rod-drop test data are presented herein.

I. INTRODUCTION

The Shield Test Experiment (STE) reactor achieved initial criticality October 9, 1961. This reactor was designed and built for use as a high-intensity neutron source for compact reactor shielding experiments. The initial physics tests on the reactor as well as the precriticality rod-drop test data are herein described. A complete facility description appears in the "SNAP Shield Test Experiment Final Hazards Summary," NAA-SR-5896,[1] while a description of the procedures used in performing the above-mentioned physics tests appears in the "SNAP Shield Test Experiment Operations Manual," NAA-SR-5897.[2]

II. SUMMARY AND CONCLUSIONS

The initial criticality for the STE reactor was achieved with 60 rejected SNAP 2 Experimental Reactor (SER) fuel rods having an average N_H of 5.69 and a total U^{235} content of 2591 gm. The second STE criticality was achieved with 56 rejected SER fuel rods having an average N_H of 5.90 and a total U^{235} content of 2471 gm plus 16 BeO rods containing a total of 7505 gm of BeO. The isothermal temperature coefficient for the system was found to have an average value between 60 and 100° F of +0.82¢/° F. The positive effect is believed to be due to the water reflector. All in-core void measurements produced negative effects while reducing the density of the water reflector resulted in a positive reactivity effect. The power and grid-plate coefficients were measured to be -0.4¢/kw and -0.4¢/° F, respectively, resulting in a 24.4¢ initial power deficit in addition to xenon, samarium and fuel-burnup effects. The most accurate determination of reactor power was the method of electrical heat substitution which yielded a reactor power of 50 ± 2 kw. The total worth of the control and safety rod system was measured to be -$8.39 ± 0.40. A mean effective prompt-neutron lifetime of 48 μsec was determined for the reactor system.

Some of the measurements performed differed from the before-the-fact physics analysis presented in the hazards summary;[1] however, the differences do not appreciably alter the conclusions reached in the report. The STE reactor has been shown to be satisfactory for the purpose for which it was designed.

III. EXPERIMENTAL TESTS

A. CONTROL AND SAFETY ROD SCRAM TESTS

The reactor transient studies described in the STE reactor hazards summary assume 70 msec are required from the time a scram signal is initiated until the control and safety rod magnets begin to release. An additional 330 msec are required for the control and safety rods to strike the snubbers and begin the snubbing action for a total scram time of 400 msec.

The experimental tests performed indicated that all 4 rods were within the total scram time of 400 msec; however, the total scram time varied from 316 to 382 msec, depending upon the particular rod. Twenty-five drop tests were performed on each rod prior to initial criticality. The measurement technique consisted of determining the instantaneous position of the rod with a precision potentiometer which was read out on an oscilloscope. A strong flexible wire was attached from the control or safety rod, being measured to a pulley on the potentiometer shaft and then to a coil spring. As the control or safety rod traveled the full 10-in. stroke, the voltage across the potentiometer varied from 10 to 0 v. The scram button on the reactor console was connected to trigger the scope sweep. For each drop test, a time photograph was made of the scope trace. In order to check the clutch-release time, exposures were made at tenfold expanded normal oscilloscope sweep. The results obtained are listed in Table I.

TABLE I

STE CONTROL/SAFETY ROD DROP TIME
(msec)

Description	Rod Release	Rod Drop	Total Scram
Control Rod No. 1	20 ± 1	296 ± 5	316 ± 5
Control Rod No. 2	49 ± 2	333 ± 7	382 ± 7
Safety Rod No. 1	20 ± 1	323 ± 10	343 ± 10
Safety Rod No. 2	30 ± 1	288 ± 6	318 ± 6

As described in the STE operation manual,[2] these tests will be repeated semi-annually, and, with the measurement of the diameter of the control and safety rods, will be used as monitors for swelling of the B_4C control and safety rods.

B. FUEL LOADING

1. Initial Fuel Loading

The initial fuel loading consisted of 60 fuel rods having an average N_H of 5.69 and a total U^{235} content of 2591 gm. In addition, the core loading consisted of 4 control/safety rod thimbles (water filled when control rods are withdrawn), 21 water-filled dummies, and 1 PuBe source element. With Safety Rod (SR) 1, SR 2, and Control Rod (CR) 2 withdrawn, a critical position of 6.18 was obtained on CR 1. This corresponded to an excess reactivity of about 26¢ at a pool-water temperature of 60° F. The initial core arrangement is shown in Figure 1.

The initial criticality calculations[1] (45 fuel elements) were based upon an N_H of 6.0. However, since this N_H was not attainable with the fuel rods that were used (rods rejected from the SER) allowance had to be made in the design of the reactor lattice for as many as 82 fuel and dummy elements to insure maximum flexibility in fuel arrangement.

2. Second Fuel Loading

The initial fuel loading arrangement was not effective for driving the STE fission plate, the purpose for which the reactor was constructed. Therefore, a second reactor loading was made, incorporating BeO reflector elements to reduce the size of the fuel loading. The second STE reactor fuel loading (the current loading) consists of 56 fuel rods with an average N_H of 5.90 and a total U^{235} content of 2471 gm. In addition, the core is reflected with 16 BeO rods containing 7505 gm of BeO, 9 water-filled dummies, and 1 PuBe source element. This core configuration (Figure 2) initially yielded a cold (60° F) clean excess reactivity of 67¢ with the thermal column in place. The reactivity worth of the thermal column graphite was measured to be +21.5¢. After several full power (50 kw) reactor runs were performed, the neutron source was removed from the system, since adequate fission products had been generated within the fuel to provide sufficient source neutrons from the (γ, n) reactions on the BeO reflector elements to satisfy the source interlock on the reactor startup instrumentation. The reactivity worth of the source in the position shown in Figure 2 was measured to be +0.6¢ with reference to a water-filled dummy which now occupies the source location, thereby bringing to 10 the number of water-filled dummies in the core.

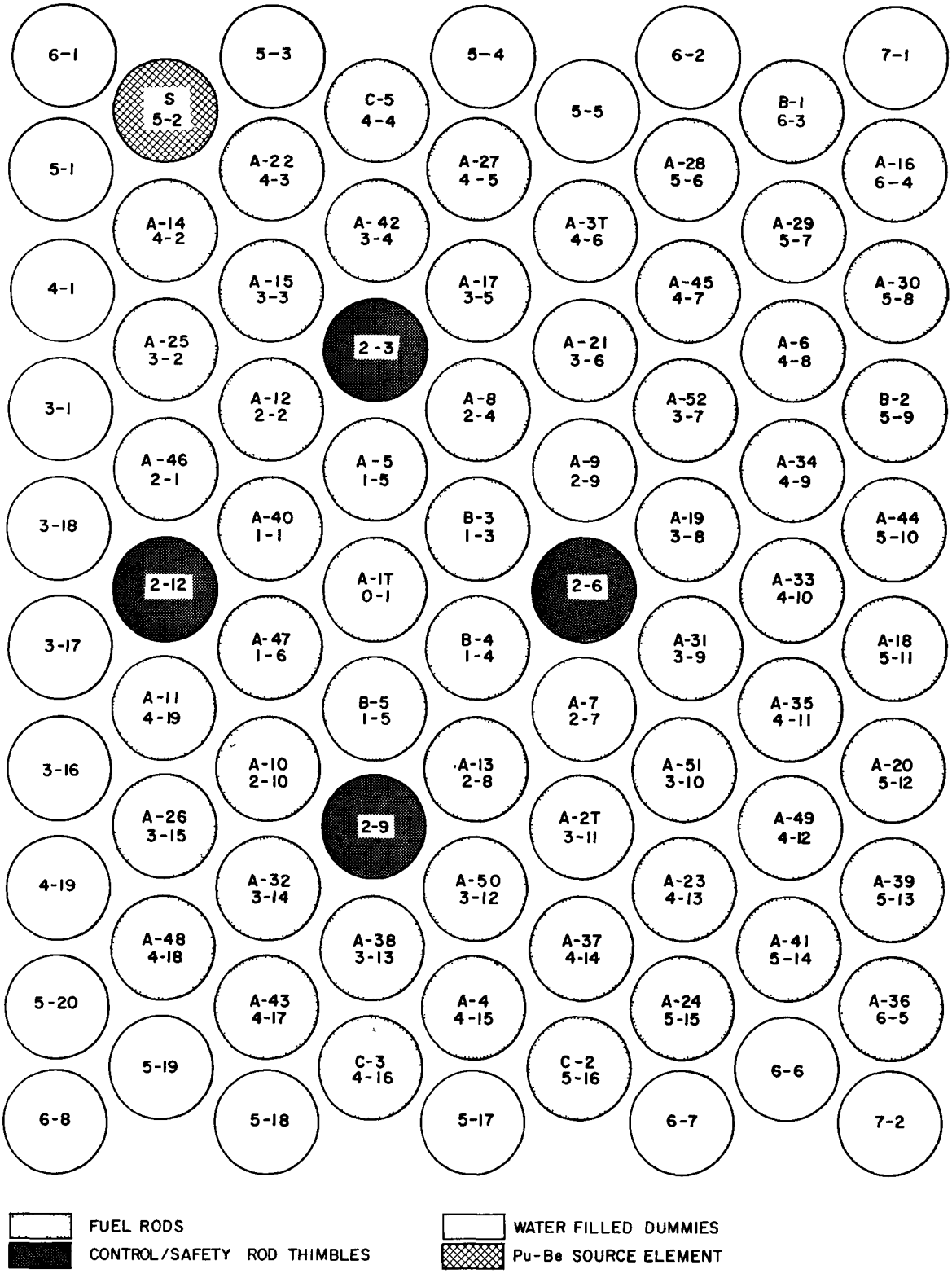

INITIAL CORE LOADING

Figure 1. Initial Core Loading

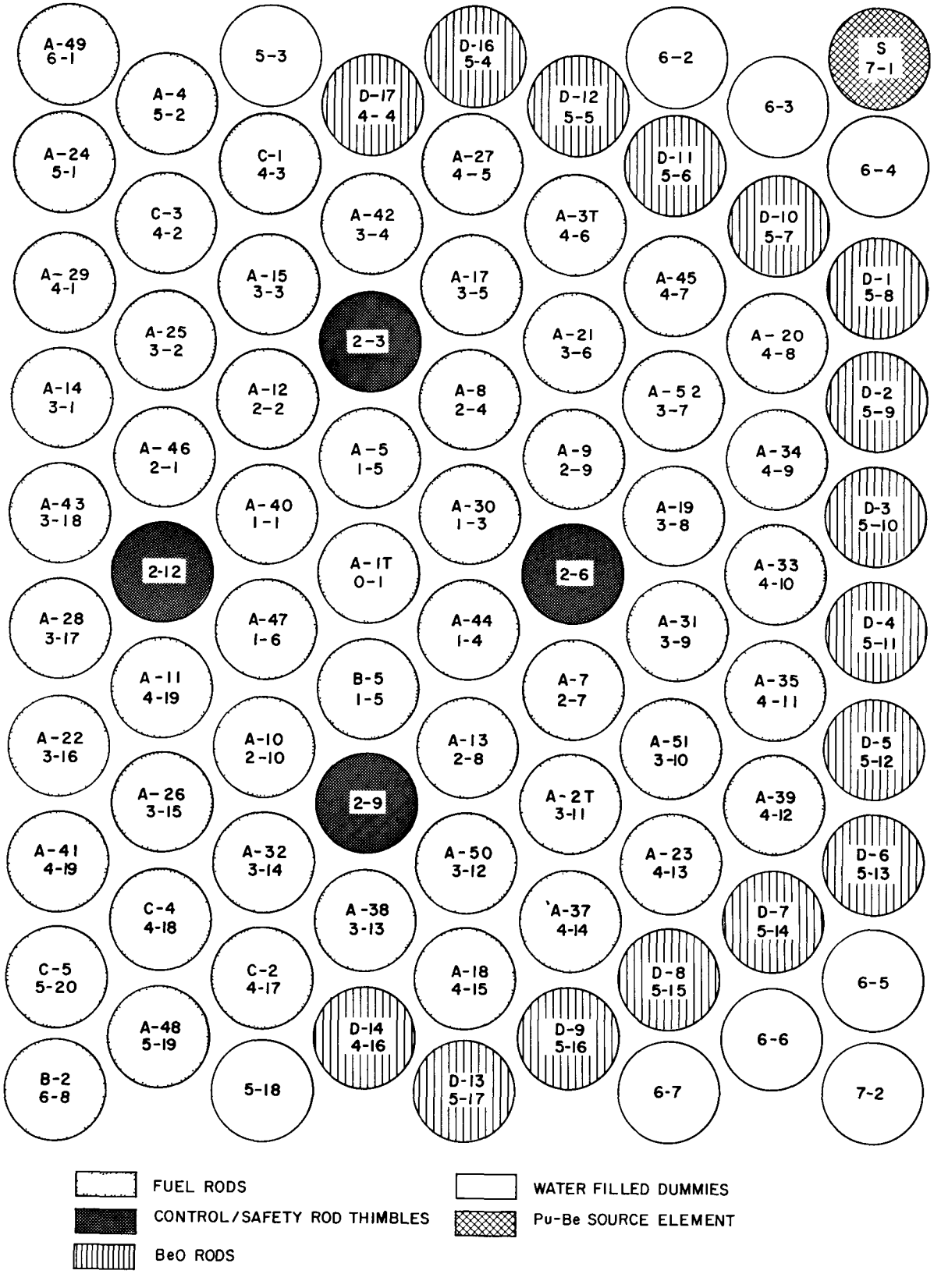

Figure 2. Second Core Loading

C. ISOTHERMAL TEMPERATURE COEFFICIENT

1. Reactor Pool

The water-filled pool that serves as a radiation shield and coolant reservoir for the STE reactor contains 3000 gal of water, and is insulated from the concrete pit in which the tank is supported by a 6-in.-thick air and gravel annulus. This water tank was used as a low-grade calorimeter for two thermal measurements: (a) power calibration of the reactor (see Section III-G), and (b) the isothermal temperature coefficient of the STE reactor which is herein described.

Two 440-v immersion heaters having a total measured power rating of 38 ± 1 kw were inserted into the pool tank, and the water was continuously circulated through the reactor core from the pool at the rate of 30 gpm, or one complete pool-water change every 100 min. While maintaining the reactor critical, using the automatic reactor controller, the temperature of the water and the fuel elements was monitored as a function of total excess reactivity in the reactor system. The water temperature was varied from 40 to 164° F during the course of the experiment. The control rods had been calibrated, using both period- and pulsed-neutron techniques (see Section III-D), prior to the temperature coefficient measurements. These measurements were performed at a reactor coolant inlet temperature of 60° F. As the water temperature of the pool tank is changed, the actual position of the poison section of the control and safety rods differs from the synchro control/safety rod position indicators, due to the thermal expansion of the rods. The discrepancy is appreciable since the control/safety rods are 18 ft in length and are composed of Al. The actual data, the expansion correction and the final isothermal temperature coefficient, are presented in Figure 3. The isothermal temperature coefficient of reactivity varies from +1.6¢/° F at 40° F to +0.14¢/° F at 160° F. The average value over the normal operating range (60 to 100° F) was determined as +0.82¢/° F. The positive coefficient could not be attributed to in-core effects since the power, grid-plate, and void coefficient measurements within the fueled reactor lattice yielded negative effects with respect to temperature increases. However, void measurements performed in the positions occupied by water-filled dummies led to positive effects (see Section III-F). Based on these results, an experiment was designed to determine if the positive effect was due to reducing the density of the water reflector as a function of temperature increase. The details of the experiment are described in the following text.

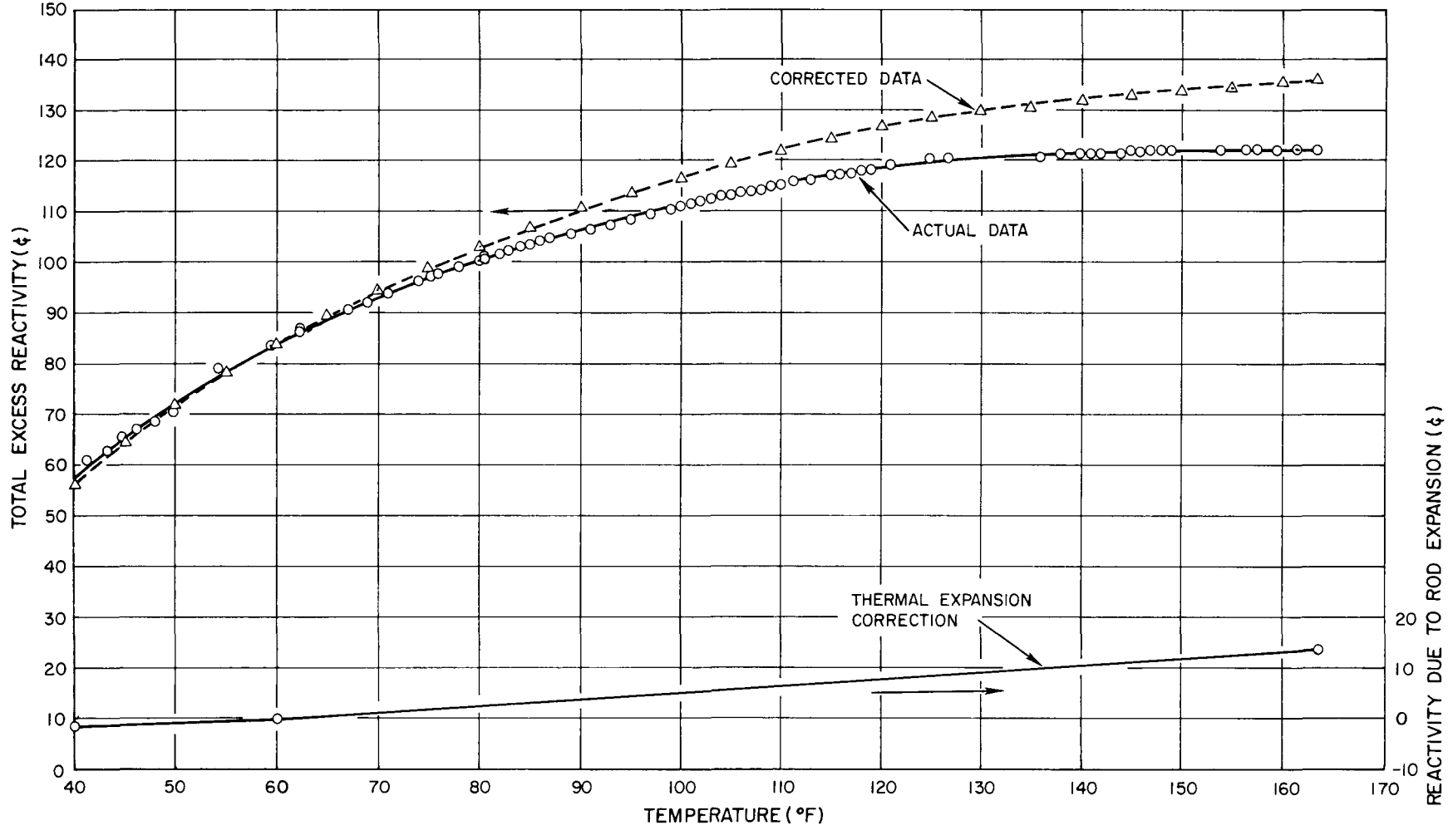

Figure 3. Measured STE Temperature Coefficient

2. Reflector Tank

An experiment was designed to evaluate the reactivity effect of heating the water reflector adjacent to the reactor core without transferring an appreciable amount of heat to the reactor proper. To achieve this result, a 4-1/2 by 16 by 17-1/2-in. ID box was constructed of 1/8-in. stainless steel. The box was covered with 1/4-in. Lucite glued with an epoxy resin, to act as thermal insulation. Six 500-w strip heaters were mounted inside the box. Steam generated by local boiling near the heaters escaped from the box through a small hole in the peak of the sloping roof of the box (see Figure 4). During the experiment the water temperature within the box, the fuel element temperature, and the reactor core inlet and outlet temperatures were monitored. The reactor was maintained critical at a power level of 10 w by the automatic controller. The reactivity was measured from a reflector temperature of 43 to 165° F. The data are presented in Figure 4. The data obtained in the experiment yield an average value of $+0.015 \pm 0.004¢/°$ F for the reactivity effect of heating the water in the reflector tank. The geometry of the experiment does not allow a direct quantitative comparison to the above-measured isothermal temperature coefficient; however, it is noteworthy that the reactivity effect, although small, is definitely positive. If it were physically possible to perform the experiment in closer proximity to the actual fuel elements, the reactivity should be even more pronounced. The closest approach on the inside of the reflector tank to an active fuel element is 2-3/4 in. Large void measurements within the core box are discussed in Section III-F.

D. REACTIVITY MEASUREMENTS

1. Technique Employed

A series of reactivity measurements were performed using positive-period and pulse-neutron techniques. The circuitry used in performing the positive-period measurements is similar to that used at other reactor installations, and is shown in block-diagram form in Figure 5.

The range of periods measured using this technique varied from 20 to 200 sec, which corresponds to excess reactivities from 25 to 5¢, respectively. The current from a boron-lined uncompensated ion chamber was converted to a voltage by a vibrating-reed electrometer. This voltage was then converted to a frequency by a voltage-to-frequency converter. The frequency was then measured by the electronic counter, counting for either 1- or 10-sec repetitive intervals, and

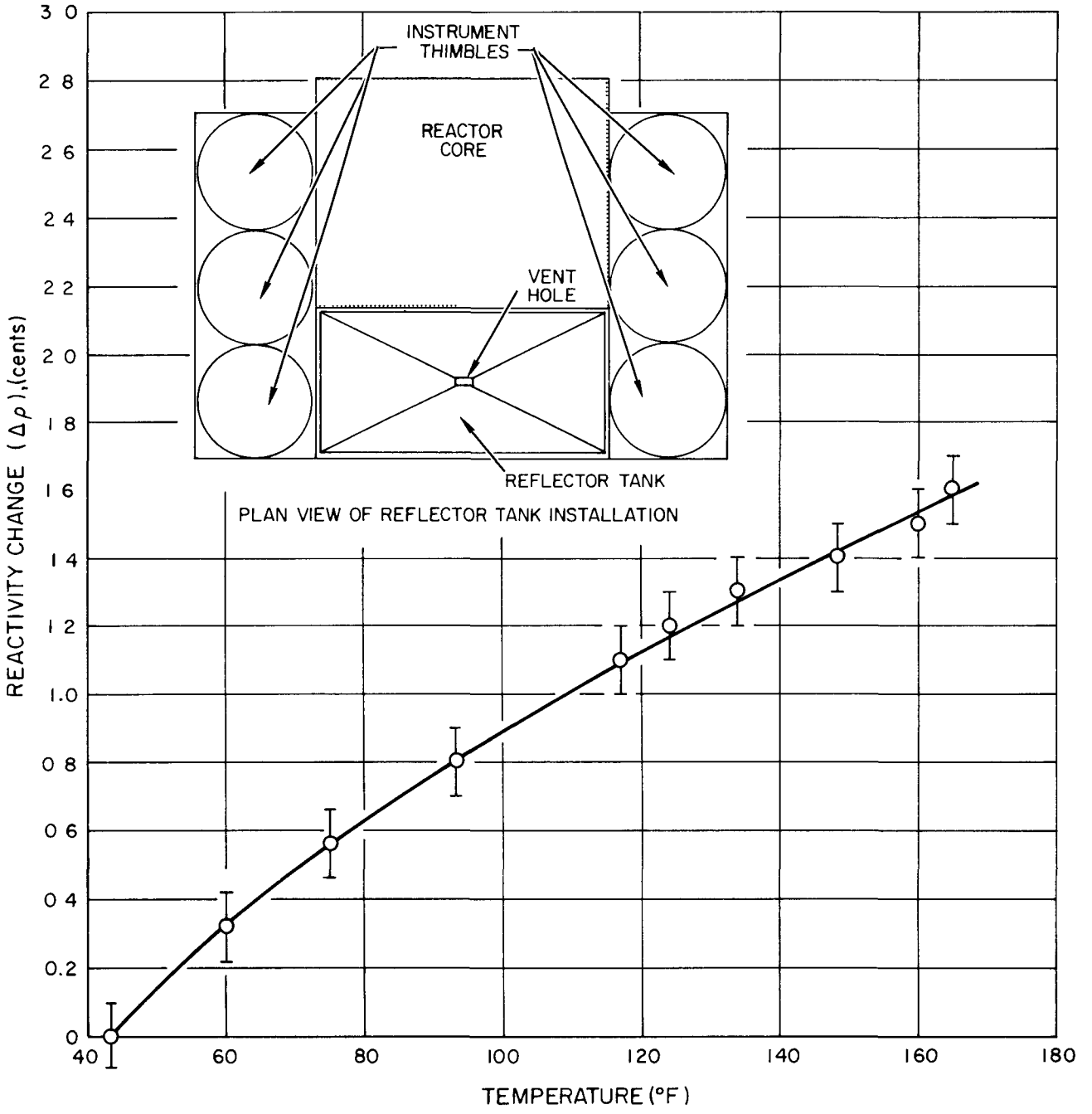

Figure 4. Reactivity vs Temperature of STE Reactor Reflector Tank

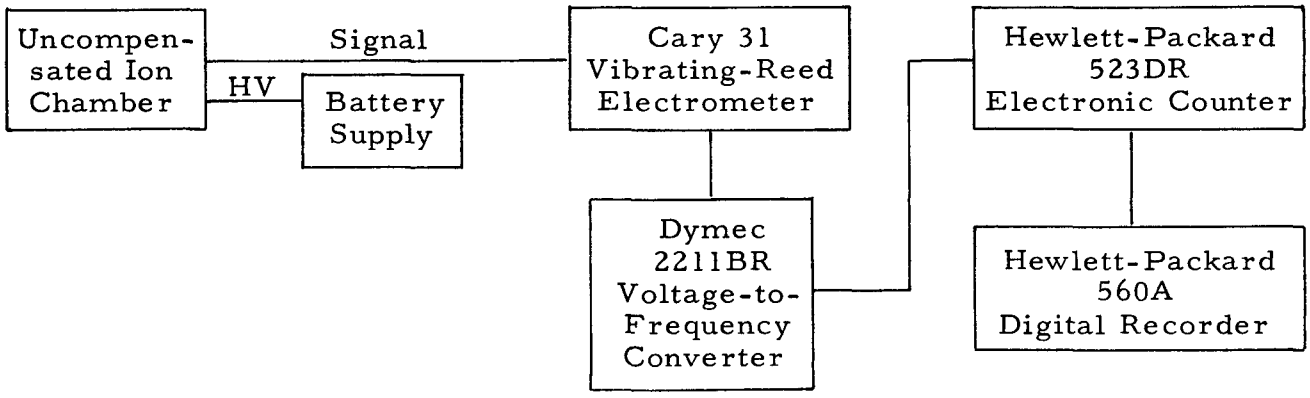

Figure 5. Positive-Period Measuring Circuit

recorded on printed tape by the digital recorder. The rising exponential obtained was then fitted by least-square techniques and a period determined. The excess reactivities corresponding to these reactor periods were then obtained from the in-hour equation, using the measured mean effective neutron lifetime of 47.9 μsec, with an assumed effective delayed-neutron fraction (β_{eff}) of 0.0079,[1] which was obtained analytically by boron substitution techniques.[3] A plot of the STE in-hour equation is shown in Figure 6.

A second technique used in obtaining STE reactor reactivity measurements was the pulse-neutron method, which consists of repetitive pulsing of a subcritical assembly with a neutron source. A multichannel time analyzer is used to record the neutron population as a function of time following each pulse from the neutron generator.

This series of experiments was performed after the STE reactor had achieved criticality and the second loading configuration had been established, but prior to insertion of the thermal-column graphite. The neutron-generator target tube was placed in the thermal column adjacent to the bismuth window on the reactor-core centerline. Four ZnS(Ag) thermal neutron detectors were placed adjacent to the bismuth window and were gamma-ray shielded with leak bricks from x-rays produced by the neutron generator. A block diagram of the instrumentation system is shown in Figure 7. The instrumentation system is essentially that used at KAPL for similar measurements.[4]

The reactivity of a reactor system is related to the mean effective prompt-neutron generation time by the following relations:

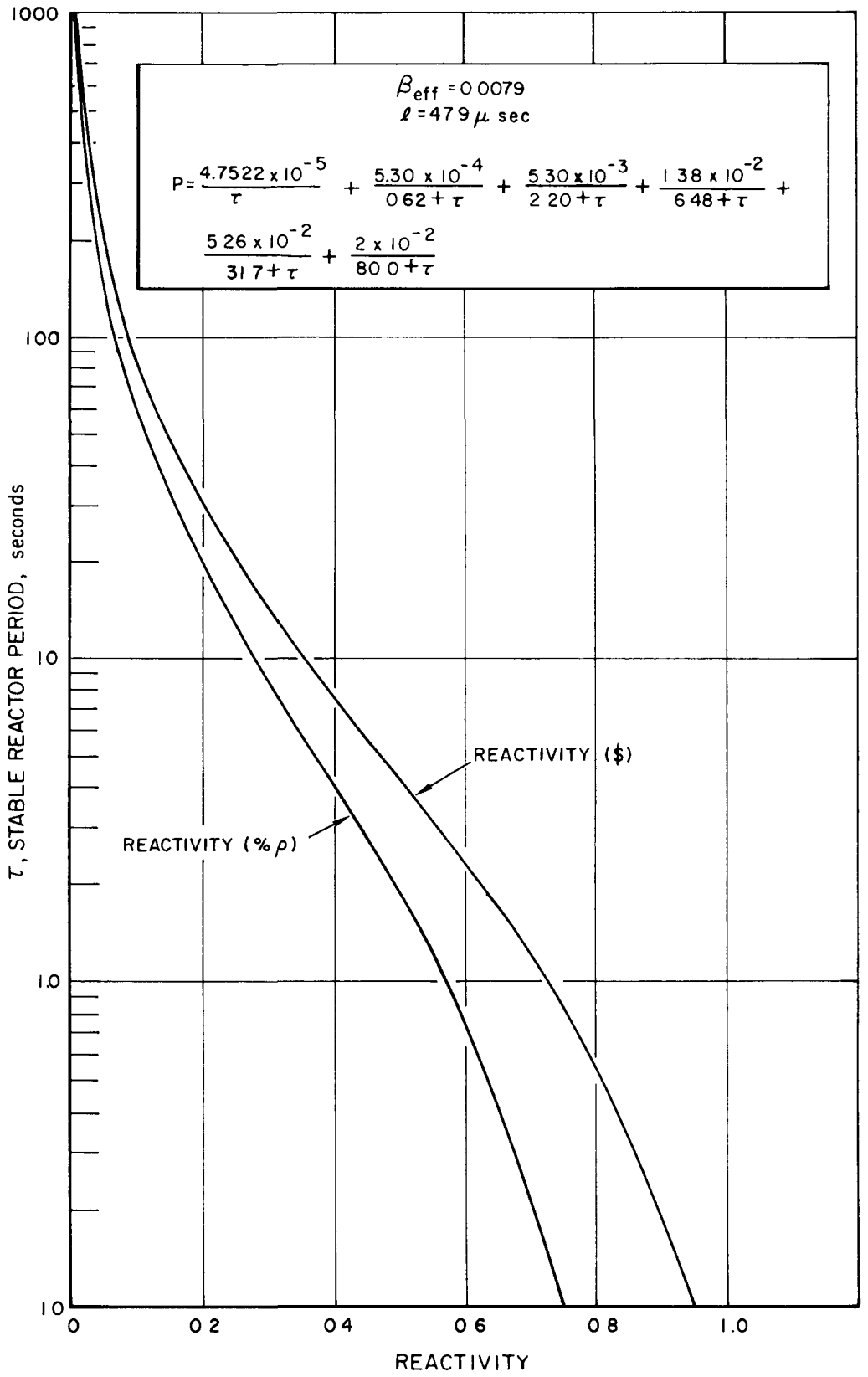

Figure 6. STE In-Hour Equation

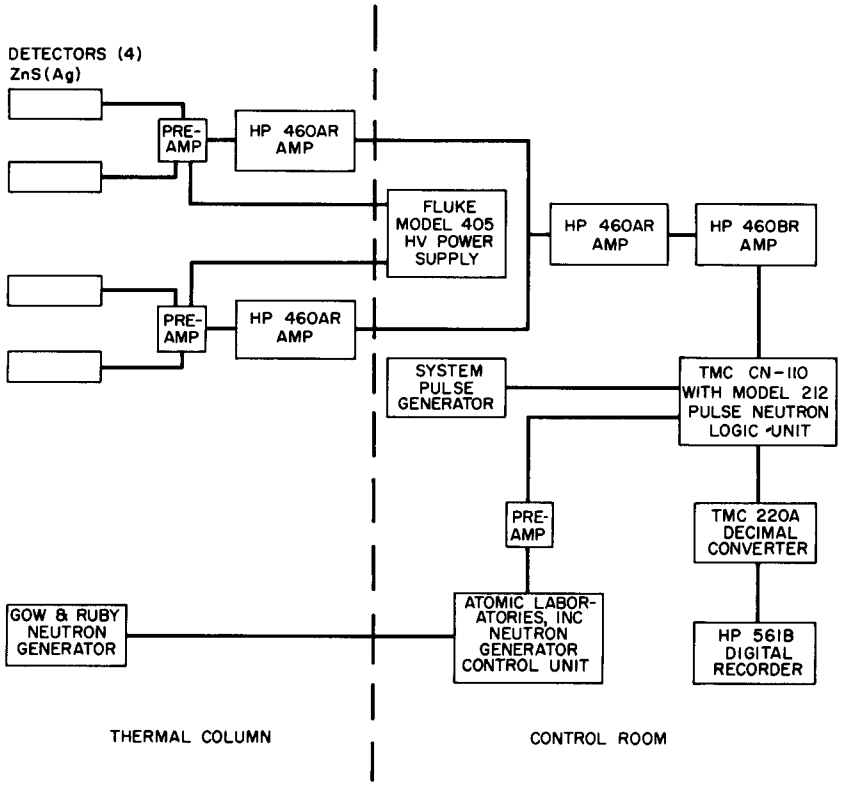

Figure 7. Pulse Neutron Circuitry

$$P = \frac{\alpha}{\alpha_c} - 1 \quad , \qquad \ldots (1)$$

where

P = subcritical reactivity ($) ,

α_c = decay constant at critical (sec^{-1}) ,

α = decay constant for measured reactivity (sec^{-1}) ,

and

$$\alpha_c = \beta_{eff} / \ell_{eff} \quad , \qquad \ldots (2)$$

where

β_{eff} = effective delayed-neutron fraction (unitless) ,

ℓ_{eff} = mean effective prompt-neutron generation time (seconds).

Upon pulsing a subcritical assembly, the short burst of neutrons creates a high neutron flux which dies out exponentially, with the fundamental mode becoming predominant. The time analyzer is so constructed that events occurring at various times after an initial event are sorted and stored in the memory of the unit. The slope of the curve of counts vs time is α, as defined in Equation 1. The true value of α is complicated by the effects of the residual delayed neutrons which are also decaying exponentially. In order to evaluate α, a least squares computer program was written which separates the slopes of the two exponentials. A typical pulse-neutron decay plot is shown in Figure 8. The details of actual experiments are described below.

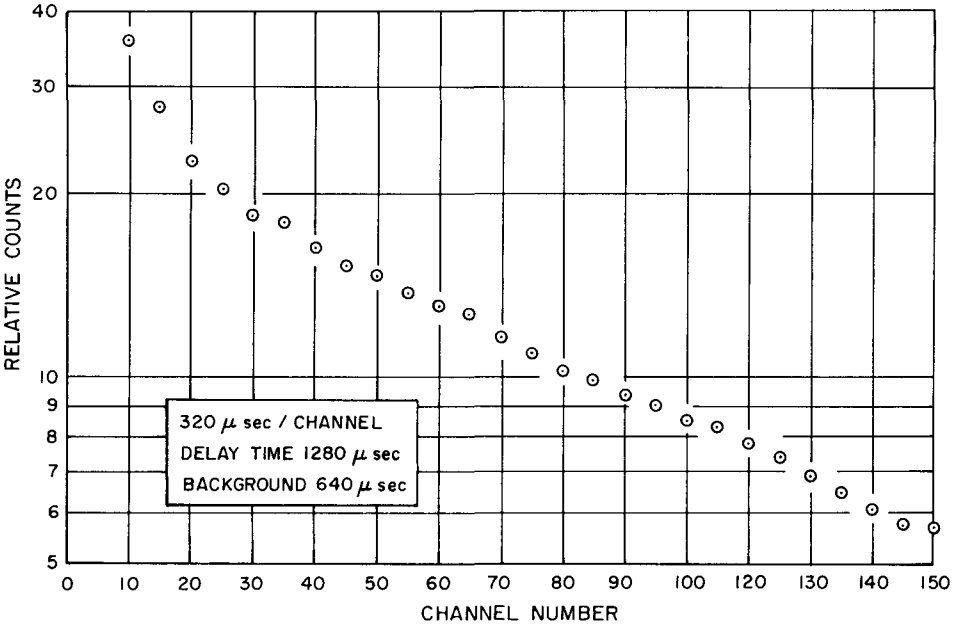

Figure 8. Typical Pulse-Neutron Decay Plot

2. Control and Safety Rod Calibrations

The large reactivity worth of the STE control and safety rod system ($8.39, total) does not allow complete calibration of any one rod using positive-period techniques, due to the 75¢ excess reactivity limitation placed upon the system for safety considerations.[1] However, as shown in Figure 9, the lower 7 in. of CR 1 was calibrated by this method. Subcritical measurements were then performed with CR 1 completely inserted to evaluate the total rod worth. The CR 1 uses stainless steel as the poison element and is used in conjunction with the automatic controller for fine adjustment of the reactor power level. The rod is identical in physical size with the other three control/safety rods, but is

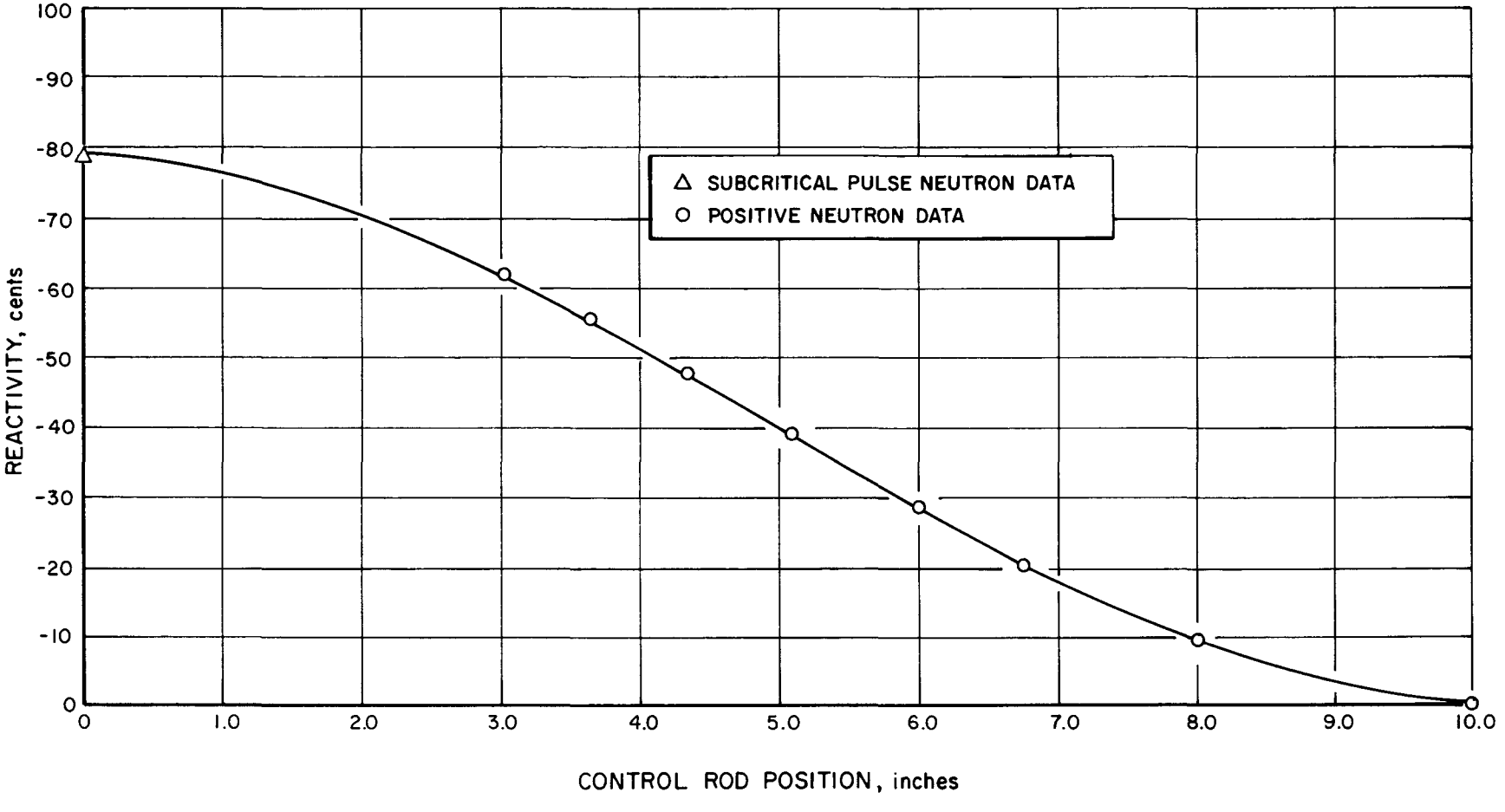

Figure 9. STE Control Rod No. 1 Calibration Curve

slightly heavier in weight, due to the difference in composition of the poison section.

Control Rod No. 2 is located in a region of lowest neutron flux of the 4 control/safety rods, and therefore has a lower corresponding reactivity worth than the other 2 safety rods which are of identical design and composition. The lower 4 in. of this rod was calibrated with positive-period techniques in conjunction with the calibration of CR 1, i.e., incremental sections of each of the rods were calibrated by shimming with one rod while evaluating an incremental section of the other. In no case did the measured periods exceed the fast-period scram limitation of 10 sec. Several data points were obtained by pulse-neutron techniques in the central region of the rod, and one measurement with the rod fully inserted. Similar individual measurements with SR 1 and SR 2 fully inserted were performed as well as a test with all rods inserted to evaluate the effect of rod "shadowing." The calibration curve for CR 2 is shown in Figure 10, while the total control/safety rod reactivity values are listed in Table II.

TABLE II

MEASURED CONTROL/SAFETY ROD REACTIVITY WORTH

Rod	Rod Worth ($)
CR-1	-0.79 ± 0.05
CR-2	-2.30 ± 0.10
SR-1	-2.62 ± 0.10
SR-2	-2.68 ± 0.10
All Rods	-8.39 ± 0.40

The fact that the sum of the individual control/safety rods yields the same reactivity value as the all-rod measurement is strictly coincidental; although the errors in the measurement are relatively small, ~5%, they indeed exist.

3. Fuel and Reflector Element Reactivity Measurements

The reactivity worth of STE reactor fuel elements was evaluated as a function of position from the vertical centerline of the fueled reactor core. The measurements were performed by removing the fuel or dummy element in question and measuring the reactivity of the system. Reactivity values < + 75¢ were

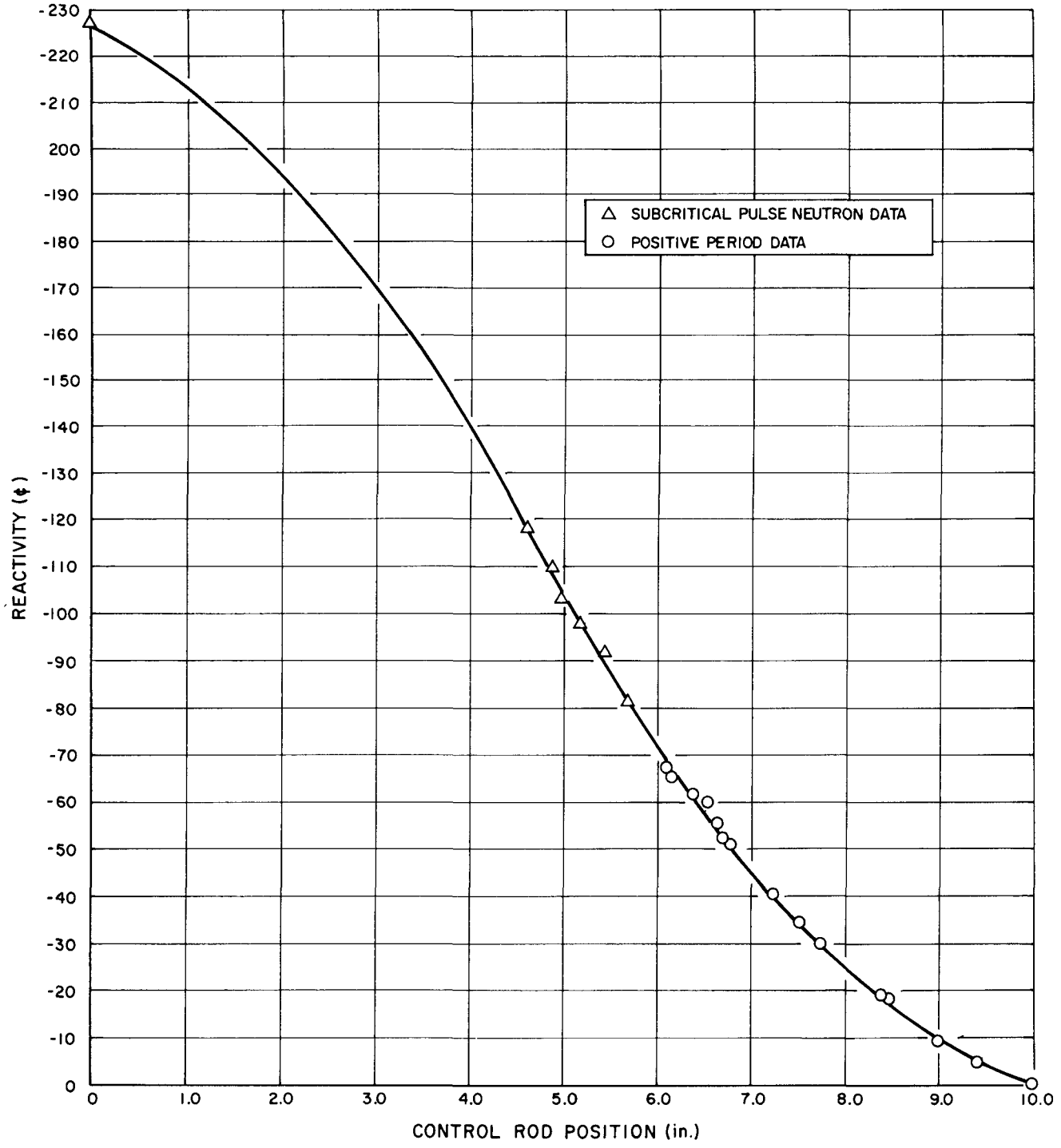

Figure 10. STE Control Rod No. 2 Calibration Curve

obtained by positive-period techniques in conjunction with the previously calibrated control rods, while reactivities >+75¢ were obtained by pulsed-neutron techniques. All measurements were performed relative to water filling the same core position. The data obtained from these measurements are listed in Table III and plotted in Figure 11 as a function of reactor-core radius. For comparison, a plot of the square of the measured relative thermal neutron flux is also presented in Figure 11.

TABLE III

FUEL/DUMMY REACTIVITY WORTH AS A FUNCTION OF CORE POSITION

Core Position	Element Removed	Element Worth (¢)
1-4	A-44	+168.0
2-8	A-13	+122.2
3-9	A-31	+85.8
3-12	A-50	+84.1
4-15	A-18	+56.0
5-15	D-8 (BeO)	+14.7
5-17	D-13 (BeO)	+11.9
6-6	D-22 (H_2O)	<±1.1
7-2	D-20 (H_2O)	<±1.1

The fuel rod reactivity agrees fairly well with the square of the thermal-neutron flux as would be expected. The reactivity effects of water-filled dummies vs a water-filled column were not measurable; i.e., the actual reactivity change resulted in a stable reactor period longer than 1000 sec.

4. Measurement of the Neutron Lifetime

The prompt-neutron lifetime of the STE reactor core was measured with pulse-neutron techniques. By referring to Equations 1 and 2,

$$P = \frac{\alpha}{\alpha_c} - 1 \quad , \qquad \ldots (1)$$

$$\alpha_c = \beta_{eff} / \ell_{eff} \quad , \qquad \ldots (2)$$

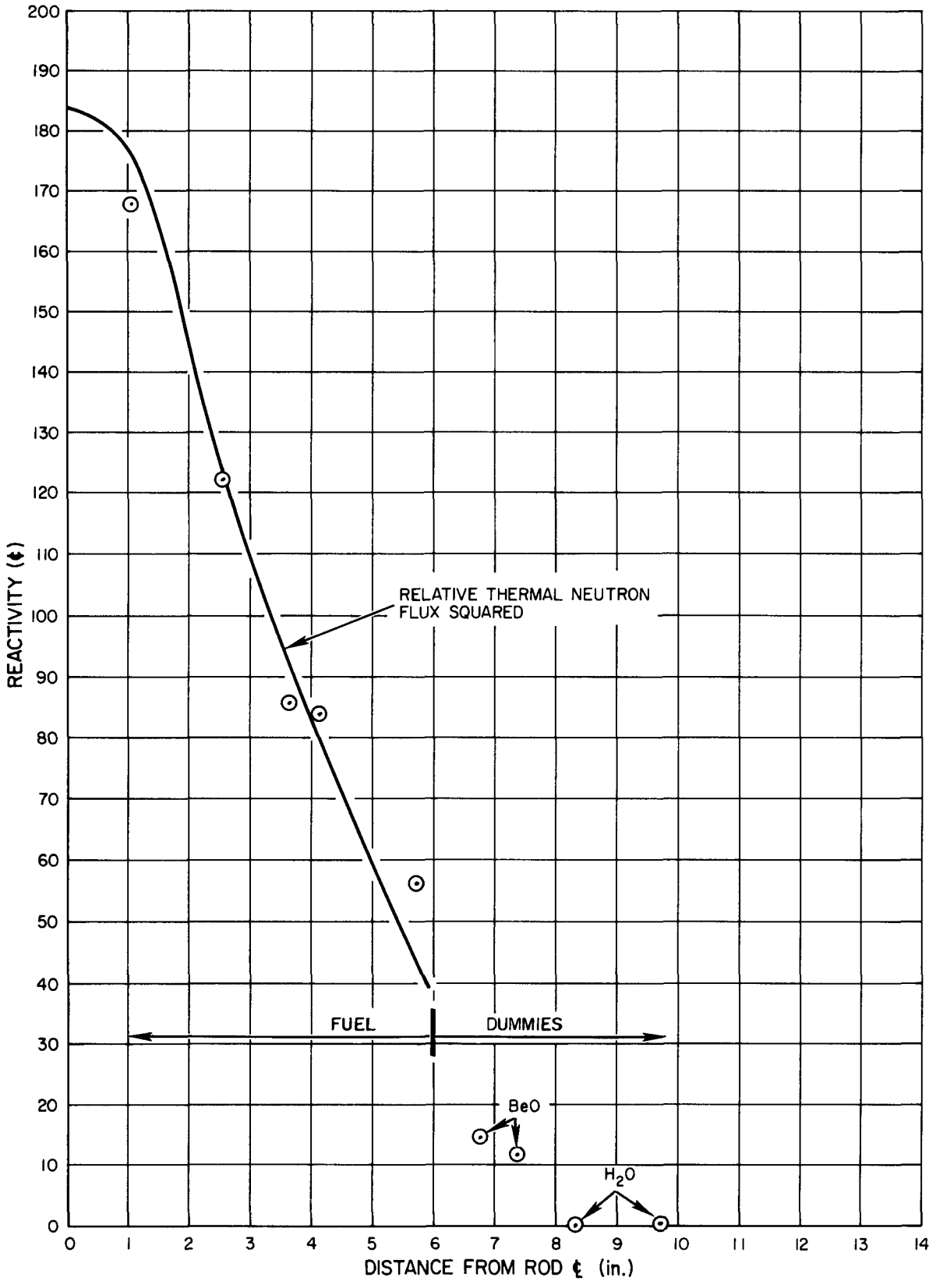

Figure 11. Fuel/Dummy Rod Worth vs Core Position

it can be seen that at critical P = O, $\alpha_c = \alpha = \beta_{eff}/\ell_{eff}$. Assuming a β_{eff} of 0.0079,[1,2] a measurement of ℓ_{eff} can be made by measuring α while maintaining the reactor at critical.

In order to maintain the reactor at critical while pulsing the reactor with the pulsed-neutron generator, cyclic operation was necessary. The reactor was pulsed until a measurable reactor period was initiated, at which time the neutron generator was turned off and control rods inserted until the initial critical position was again established and the neutron pulsing was again started. This process was continued until sufficient data were accumulated for the necessary statistics. A value of $1/\alpha_c$ of 6069 μsec was obtained in these measurements corresponding to

$$1/\alpha_c = \ell_{eff}/\beta_{eff} = 6069\ \mu\text{sec} \quad ,$$

$$\therefore\ \ell_{eff} = (6069) \cdot (0.0079) = 47.9\ \mu\text{sec} \quad .$$

This compares with the theoretical value of 30 μsec.[1,2]

5. Reactivity Worth of the Thermal Column

Upon completion of the pulsed-neutron reactivity measurements, the pulsed-neutron generator, detectors and amplifiers were removed from the thermal column. The thermal column was then loaded with reactor-grade graphite and the reactivity effects upon the reactor evaluated by establishing criticality and measuring the resultant reactivity effects with the calibrated control rods. The addition of the graphite increased the reactivity of the reactor system by +21.5¢.

E. IN-CORE THERMAL NEUTRON FLUX TRAVERSES

Thermal neutron traverses were performed within the reactor core, using 5-mil-thick circular gold foils with a diameter of 1/4 in. One fuel element and one dummy element were modified in such a manner as to allow the thermal-neutron flux to be measured at the surface of the fuel on the centerline, and axially along the centerline of the summy element. The gold foils were contained in 20-mil-thick cadmium and aluminum boxes. The foils and foil counters were inter-calibrated with the Oak Ridge National Laboratory (ORNL) high-pressure ion chamber and the ORNL Standard Graphite Pile.[5] The gold-foil

measurements were corrected for flux depression and self shielding, using the experimental data obtained at ORNL[6,7] for gold foils exposed in water. The foil activities were then determined, using a NaI(Tℓ) scintillation spectrometer having a 2-in. diameter crystal.

An east-west thermal-neutron plot across the reactor core is shown in Figure 12. It can be seen that the thermal-neutron flux tends to peak east of the center of the fuel loading. This can possibly be explained by the combination of two effects: (1) the depression due to a strong control rod positioned at 4.2 in. west of the center of the fuel loading, and (2) the good reflection characteristics of the BeO on the east side of the core vs the poor lead and bismuth reflector located on the west side of the core. A radial flux plot from the center of the fuel loading to the south edge of the reactor core is shown in Figure 13. No flux traverse was performed from the center of the fuel loading to the north edge of the reactor core, since it was felt that due to the symmetry of the loading such a traverse would only duplicate the data presented in Figure 13 within the error of the experiment.

The uncertainty in position of the data points within the reactor core arises from the construction of the modified fuel element which, like all of the fuel and dummy elements, is held in the core box by a double-lead Acme thread attached to the bottom of the fuel element. An uncertainty thus arises in the angular position of the rods, since the foils were attached to the outside of the fuel cladding. Since the foils were located on the centerline of the dummy element, no such position uncertainty exists in the reflector points.

The measured radial peak-to-average thermal-neutron flux in the reactor core was measured to be 1.62 vs a calculated 1.13,[1] and 1.18 vs a calculated 1.09[1] for the axial direction. This leads to a volumetric peak-to-average thermal flux of 1.91, a reasonable value for this size and type of reactor.

F. VOID MEASUREMENTS

1. Fuel/SS Dummy Element Annulus Measurements

The effects of an annular void on the reactivity of the STE reactor as a function of fuel element position was experimentally determined. Fuel Element A-6, which was used during this experiment, has an N_H of 3.2 vs the second fuel loading average of 5.9. Because of this radical difference in N_H, the effect of this fuel rod as a function of core position was of interest, and was used as a normalizing point in the succeeding void measurements. The reactivity effects

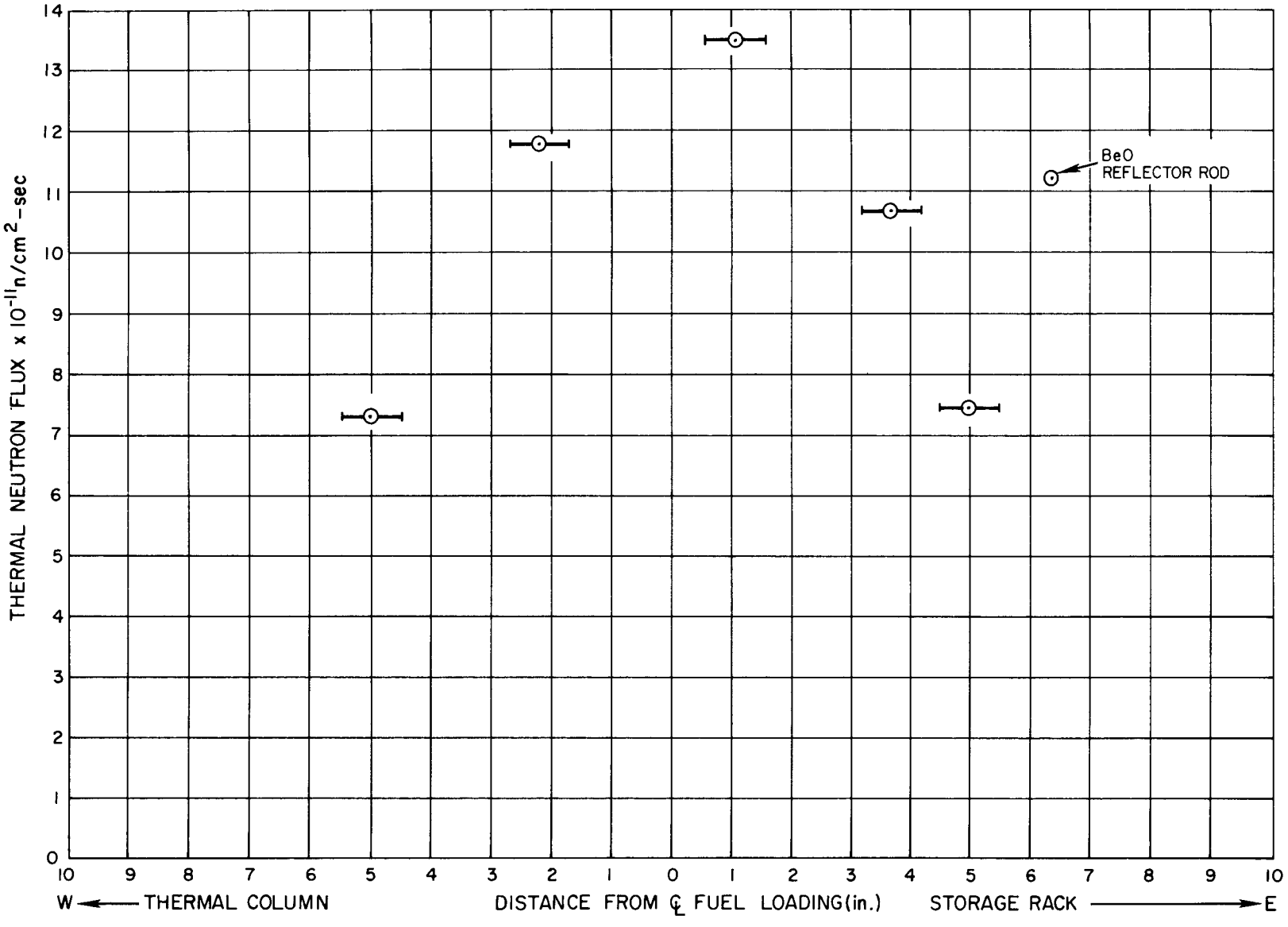

Figure 12. East-West Thermal Neutron Distribution in the STE Reactor Core at 50 kw

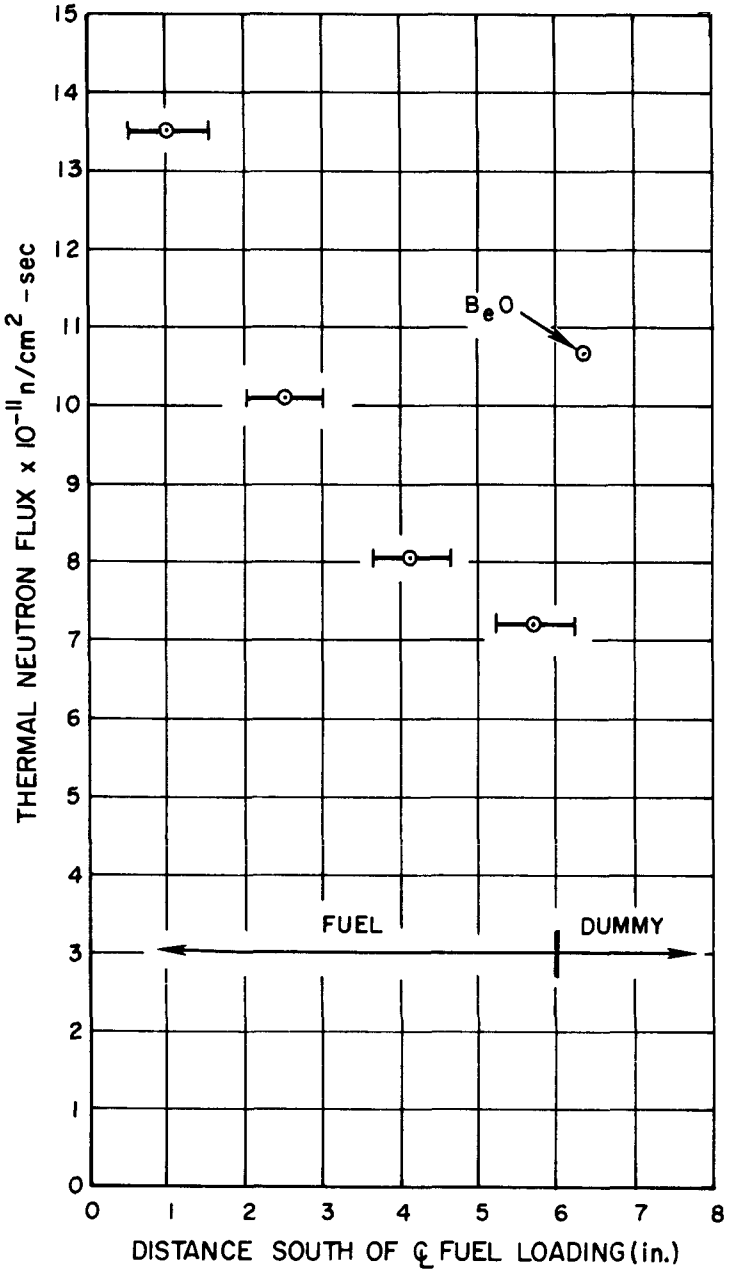

Figure 13. Centerline-South Thermal Neutron Distribution in the STE Reactor Core at 50 kw

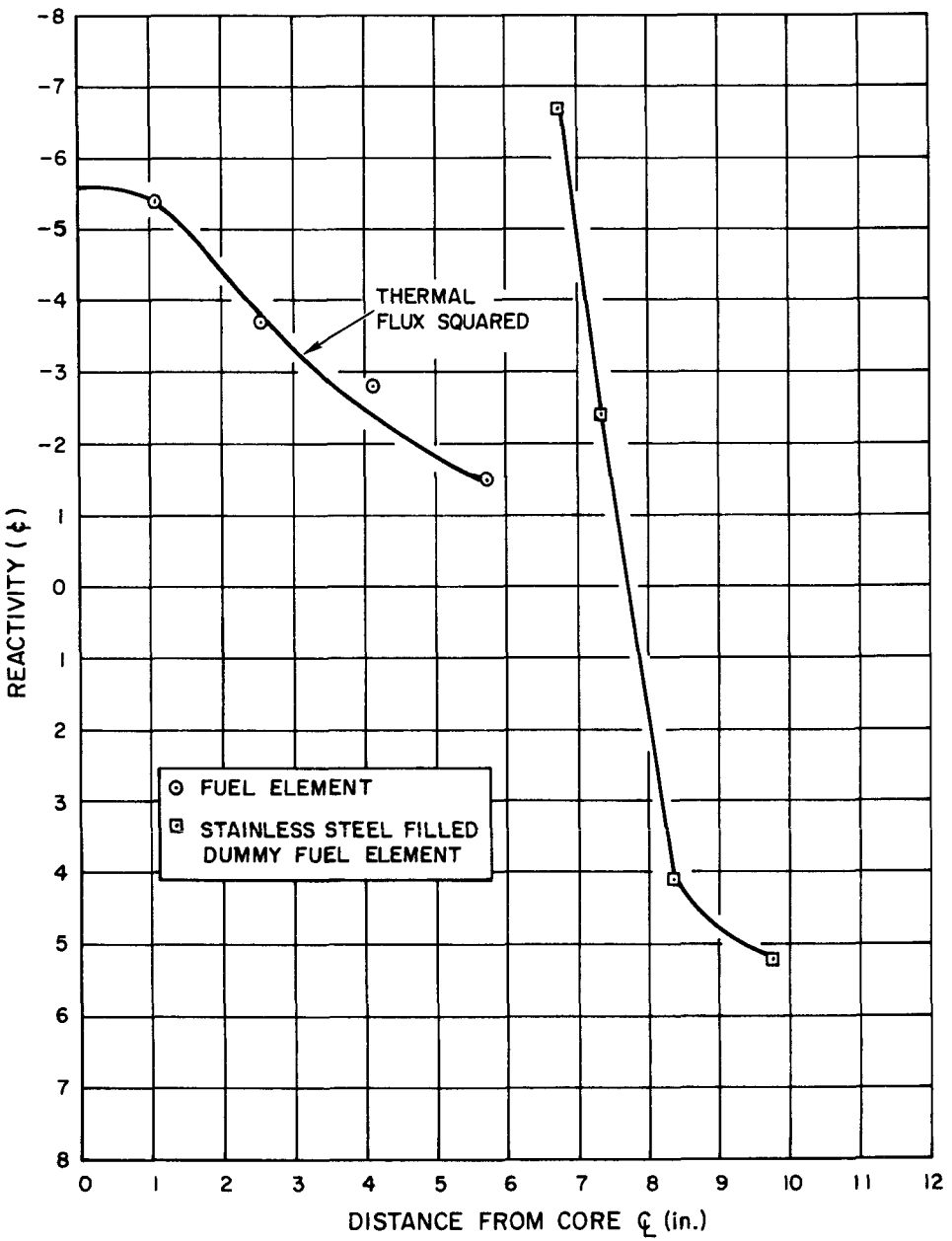

Figure 14. Reactivity of a Void Fuel/Dummy Element Coolant Annulus as a Function of Core Position

of A-6 relative to the fuel elements it replaced in the reactivity traverse are listed in Table IV.

By plugging the inlet and outlet coolant annulus of Fuel Element A-6 with small rubber stoppers, the reactivity effect of an air annulus relative to a water annulus could be measured. These data are also listed in Table IV and plotted in Figure 14. The void volume per fuel element consists of ~57 cm^3.

The annulus measurements were repeated, using a dummy fuel element identical to Fuel Element A-6, with the exception that the zirconium hydride was replaced by stainless steel. The measurements created a large thermal flux perturbation in the reactor core, but it is noteworthy that the annular air void yielded a positive reactivity effect in the STE reactor reflector with reference to water. These data are also presented in Figure 14.

TABLE IV

REACTIVITY EFFECT OF A VOID FUEL ELEMENT COOLANT ANNULUS

Core Location	Element Removed	Element Worth Relative to A-6 (¢)	Void Annulus (¢)
1-4	A-44	+16.5	-5.4
2-8	A-13	+14.9	-3.7
3-12	A-50	+8.2	-2.8
4-15	A-18	0	-1.5

2. Dummy Element – Water

The effect of large voids in the fuel region and reflector was investigated by inserting a void dummy element in the reactor at several positions and using positive-period techniques. The measurement was performed to evaluate the reactivity effects in core boiling and the influence of such boiling on the nuclear safety of the system. Measurements were made by plugging holes in a standard water-type dummy element creating a large air void of ~185 cm^3. Measurements were made with and without water in the dummy element to measure the effect of the air void on the reactivity of the system. Unfortunately, no measurements were made in the two central core positions due to the large reactivity swings involved, ~$1.85 and $1.35, respectively. (With the thermal column filled with

graphite, no means was easily available to use pulse-neutron reactivity measuring techniques.) The effect of the large void is most appreciable where the thermal-neutron flux peaks in the reflector region, as is shown in Figure 15. Voids of this size create a large perturbation of the neutron flux in the reactor core.

G. POWER CALIBRATION

Three techniques were employed to evaluate the actual power generation of the STE reactor: (1) thermal flux integration, (2) coolant flow and Δt measurements, and (3) calorimetric – all of which are described in the following text.

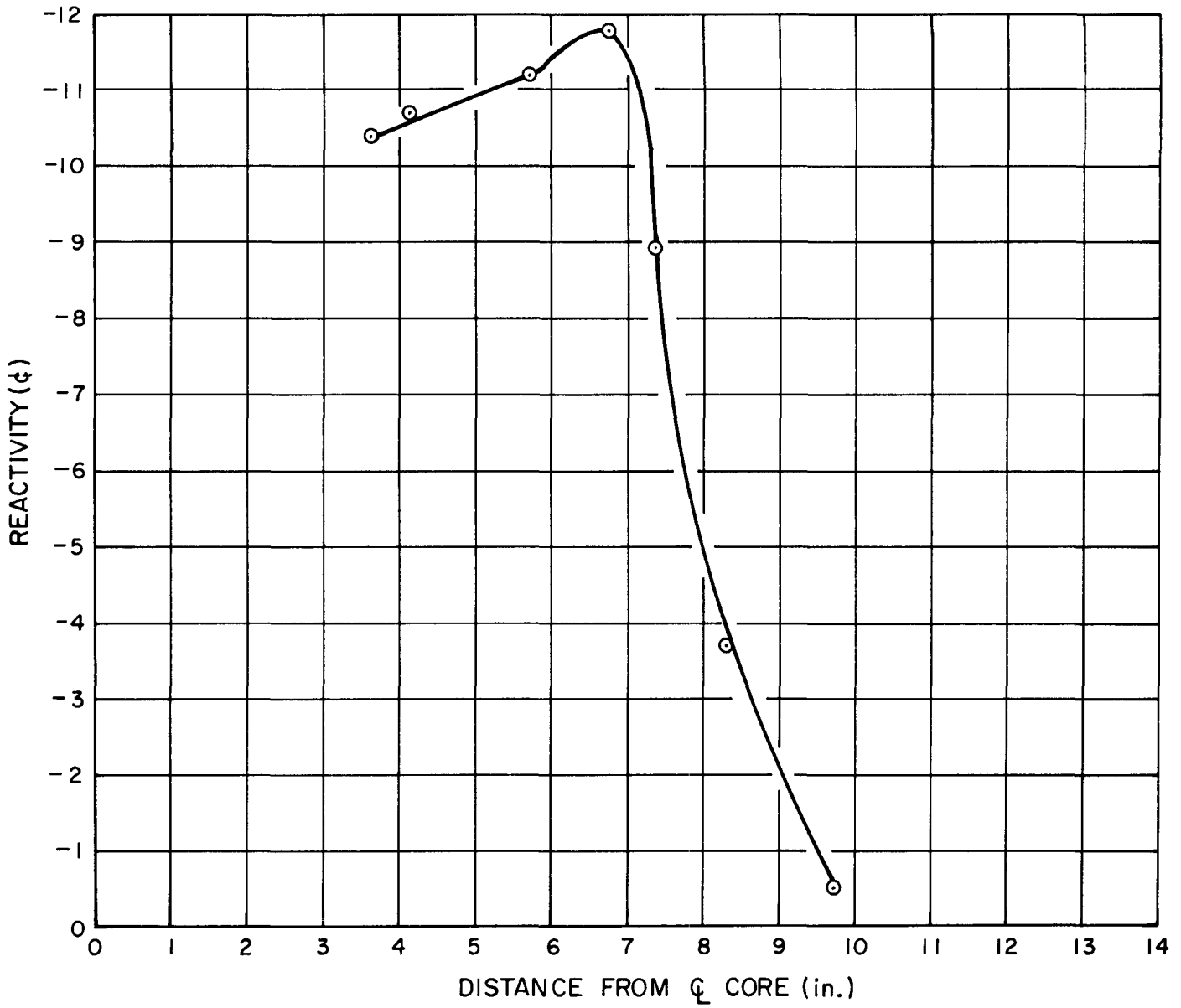

Figure 15. Reactivity Effects of a Large Void as a Function of Core Position

1. Thermal Flux Integration

Using the thermal flux traverse data obtained in Section III-E, a volumetric flux average was obtained for the STE reactor core. Since the thermal flux data were obtained at the surface of the fuel cladding, data corrections were necessary before the reactor power level could be determined. Calculations performed by Rhoades[8] indicate a factor of close to 1.41 lower average thermal-neutron flux in the fuel over that measured at the surface of the fuel as a result of a cell calculation performed on the STE reactor. After correcting for this effect, the primary sources of error in the measurement are due to the uncertainty in detector position of the foils, and the errors associated with the foil calibration. These errors have been estimated to contribute about a 20% uncertainty to the power calculated from the measured thermal-neutron fluxes. Applying the corrections determined by Rhoades leads to a power level of 54 ± 11 kw, using the thermal flux intrgration technique.

2. Coolant Temperature Rise Across Reactor

The design of the STE reactor does not allow easy reactor power determination through measurement of the coolant flow rate and temperature rise across the core. However, the total flow rate, bulk inlet temperature, and the exit coolant temperatures from the individual coolant channels at the top of each fuel element were determined by using a special thermocouple probe. By maintaining the reactor power constant, temperature traverses were obtained across the reactor core. By weighting the coolant temperature rise across the core according to fuel element coolant channel flow area as a function of distance from the center of the reactor core, an average Δt for the system was obtained. Using measured data, an expression was obtained that could relate the measured Δt of any fuel element to the average Δt for the reactor. The errors associated with the measurement of coolant temperature and flow lead to an uncertainty in the power level determination of about 20%. The reactor power level was calculated to be 51 ± 10 kw.

3. Electrical Heat Substitution

The most accurate method of reactor power level determination was found to be electrical heat substitution.

The reactor pool tank, containing 3,000 gal of water, is well insulated on the bottom and sides by a 6-in.-thick gravel and air annulus; this annulus separates the pool tank from the 18-in.-thick concrete pit which serves as a secondary

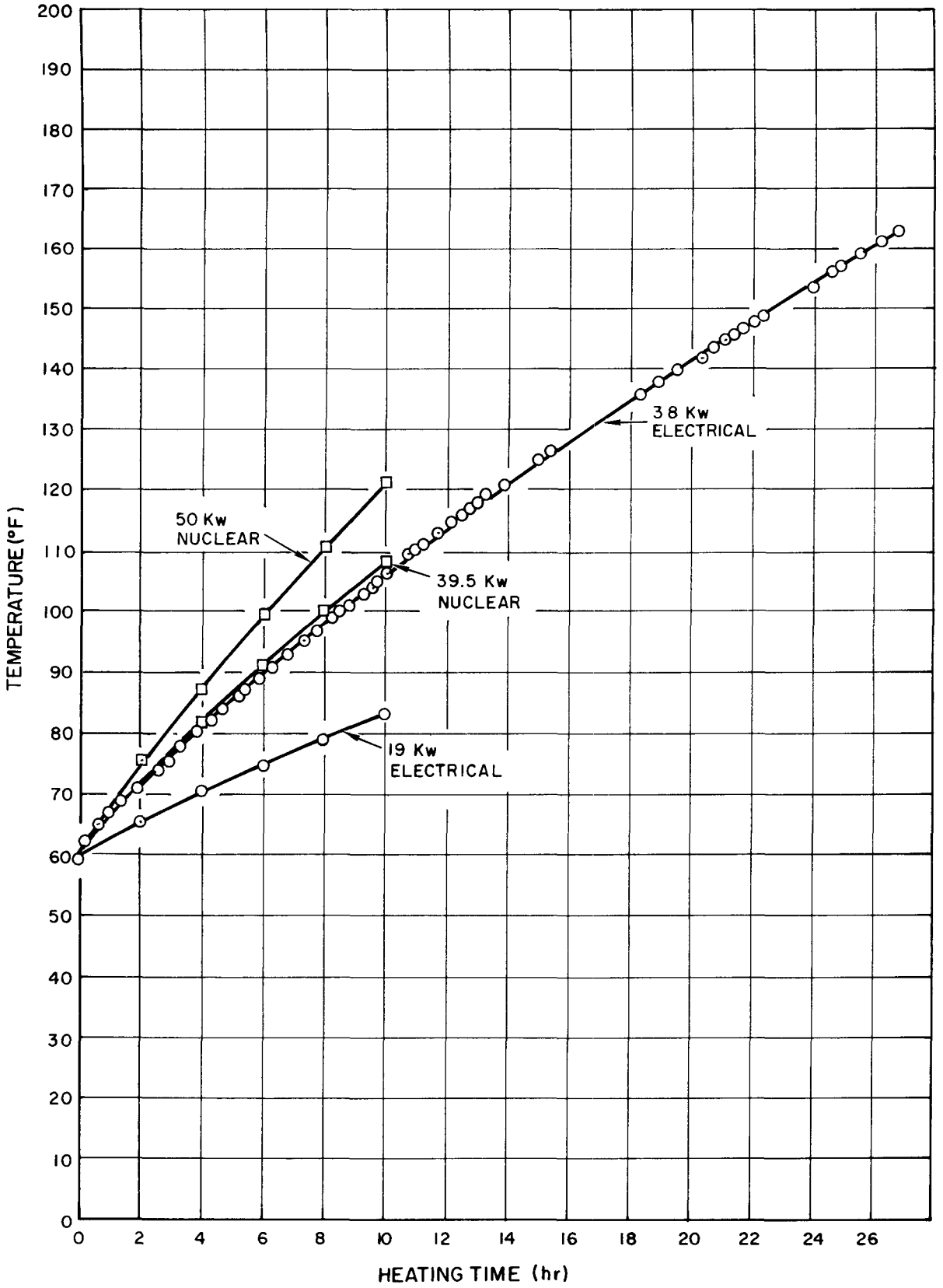

Figure 16. STE Reactor Power Calibration Curve

containment vessel and reactor support structure. By insulating the top of the pool tank and inserting electrical immersion heaters into the water, the rate of rise of the pool water temperature as a function of time for a known amount of electrical power was determined, using the procedures outlined in Section III-C of the STE operations manual.[2] Two such electrical runs were performed. Two 440-v immersion heaters were used in the first run, which extended over a period of 27 hr, coincident with the isothermal temperature coefficient measurements described in Section III-C of this report. The second electrical run used one of the 440-v immersion heaters, thereby reducing the heat input to the pool tank from 38 to 19 kw. The current and voltage to the heaters were recorded hourly, and showed no significant change over the course of the measurements. Following each run, the water in the pool tank was cooled to 60° F prior to starting the next experiment. After the two electrical runs had been completed, the heaters were removed and the reactor was raised to a power in the range of the 38-kw electrical run, using the data obtained from the second power level determination technique, i.e., by measuring flow rate and coolant Δt across the reactor core. By extrapolating the data from the two electrical runs, the power of the first nuclear run was determined to be 39.5 kw. With these data, the procedure was repeated for an estimated 50 kw by linear extrapolation of the reactor control instrumentation readings, based on the measured value at 39.5 kw.

The temperature vs heating time data for the two electrical and the two nuclear heating tests are shown in Figure 16. The uncertainty in the electrical substitution technique, including errors in instrument calibration and drift during the measurement, amount to ~4%. Therefore, the full power of the STE is 50 ± 2 kw.

A summary of the three techniques is listed as follows:

Technique	Result
1. Thermal flux integration	54 ± 11 kw
2. Coolant temperature rise	51 ± 10
3. Electrical substitution	50 ± 2

All the measurements appear to be consistent within the expected errors of the measurements performed.

H. POWER AND GRID-PLATE COEFFICIENT MEASUREMENTS

1. Coefficient Measurements

The measurements of the STE reactor power and grid-plate coefficients were performed by varying the reactor power level in steps from 0 to 50 kw, and by varying the coolant flow rate at each step in power. Reactivity measurements were obtained at each step in coolant flow rate and power. By cross plotting the measured reactivity as a function of reactor power and Δt across the core, grid plate and power coefficients can be separated analytically (see Figure 17).

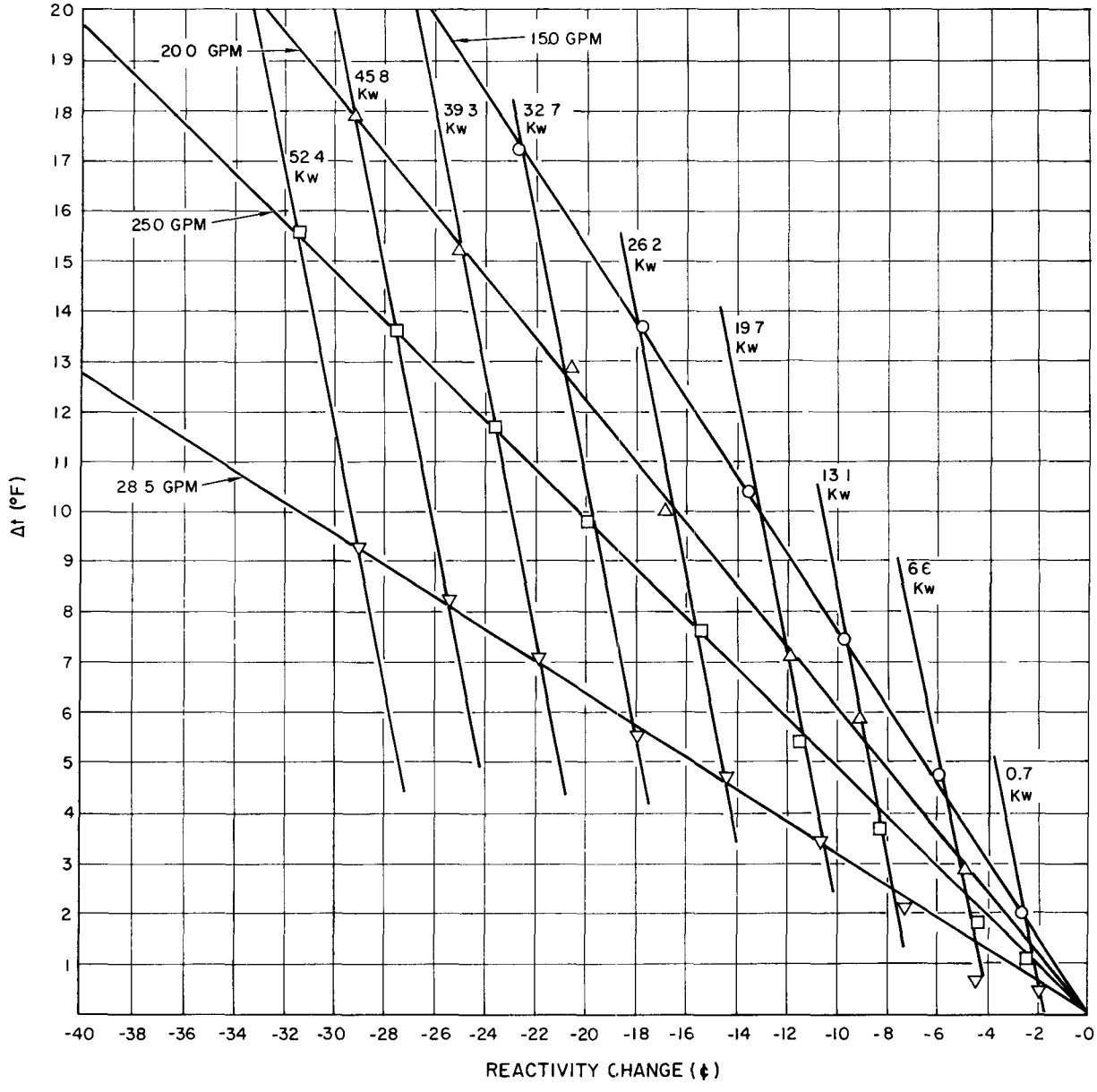

Figure 17. Reactivity as a Function of Reactor Power and Coolant Δt

The best fit of the measured data yielded values of $-0.4 \pm 0.1¢/kw$ and $-0.4 \pm 0.1¢/°F$ for the power coefficient and grid plate coefficient, respectively. The reactivity data were obtained by using the control rod calibration curves, and were corrected for the reactivity effects induced by the temperature coefficient of the system.

2. Fuel Temperature Measurements

Fuel Element A-1T was placed at four different locations within the reactor lattice. This fuel element was specially constructed with three stainless steel clad thermocouples located at three different radial positions on the axial centerline of the fuel element. Temperature measurements within the fuel were then obtained at a power level of 50 kw. These data are presented in Figure 18. In order to obtain a mean fuel temperature for the reactor fuel, the temperatures measured in the fuel were volumetrically weighted, using an axial peak-to-average ratio proportional to the thermal-neutron flux, i.e., 1.18. These mean values for the four core locations were then plotted as a function of reactor core radius, and are shown in Figure 19. By again volumetrically weighting these values, a mean fuel temperature of 103°F above coolant inlet temperature was obtained.

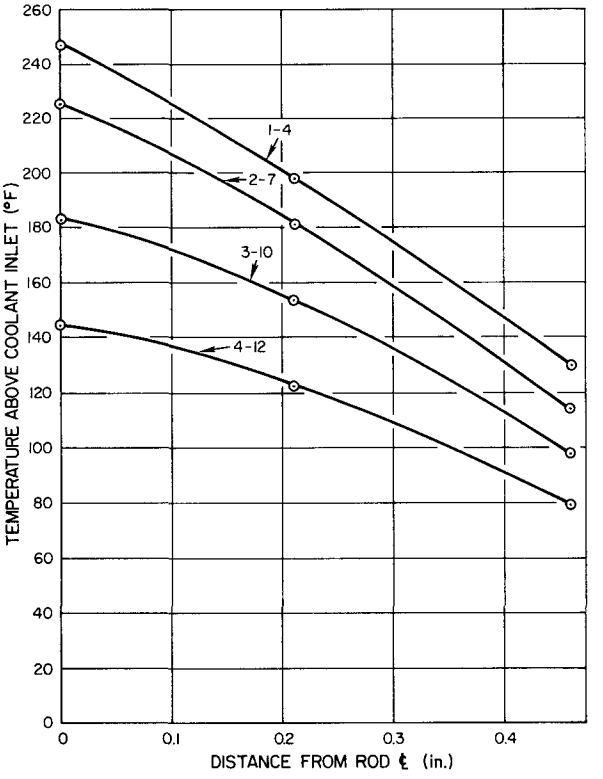

Figure 18. Radial (℄) Temperature Distribution in STE Reactor Fuel Rods at 50 kw

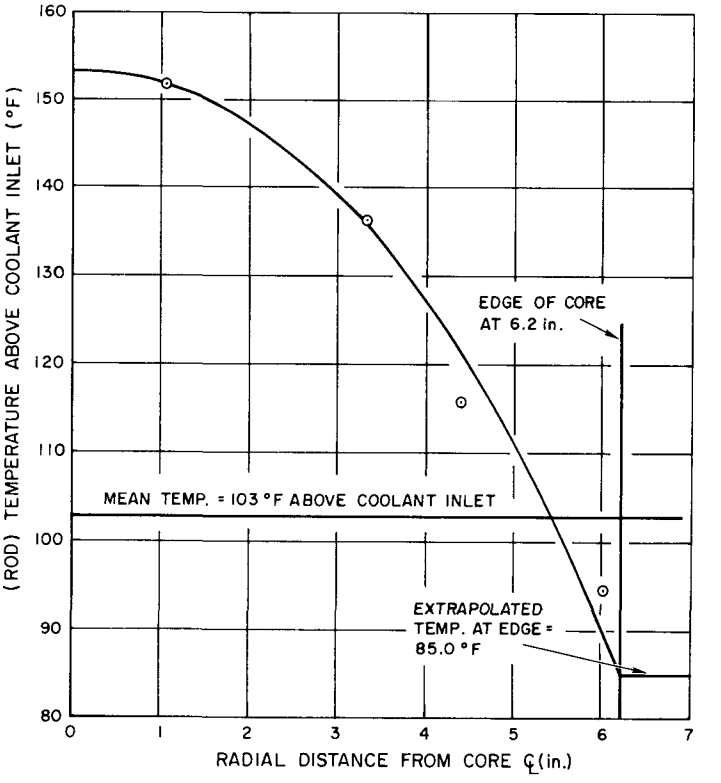

Figure 19. Volume-Weighted STE Fuel Element Temperature as a Function of Core Position

REFERENCES

1. R. L. Tomlinson, "SNAP Shield Test Experiment Final Hazards Summary," NAA-SR-5896, March 1961

2. R. P. Johnson "SNAP Shield Test Experiment Operations Manual," NAA-SR-5897, June 1961

3. T. F. Ruane, et al., Trans. Am. Nuc. Soc. 1(2) 142 (1958)

4. B. E. Simmons and J. S. King, "A Pulsed Neutron Technique for Reactivity Determination," Nuclear Sci. and Eng. 3, 595-608 (1958)

5. G. M. Estabrook, "Neutron Physics Division Annual Progress Report, September 1, 1960," ORNL-3016, p 129, 130

6. W. Zobel, "Neutron Physics Division Annual Progress Report, September 1, 1960," ORNL-3016, p 267-269

7. S. A. Hasnain, T. Mustafa, and T. V. Blosser, "Neutron Physics Division Annual Progress Report, September 1, 1961," ORNL-3193, p 78-94

8. W. A. Roades, Atomics International, personnal communication